

## SLIM DISK MODEL FOR ULTRA-LUMINOUS X-RAY SOURCES

KEN-YA WATARAI<sup>1,3</sup>, TSUNEFUMI MIZUNO<sup>2</sup>, SHIN MINESHIGE<sup>1</sup>  
2000/11/23 *ApJL* accepted

## ABSTRACT

The Ultra Luminous X-ray Sources (ULXs) are unique in exhibiting moderately bright X-ray luminosities,  $L_x \sim 10^{38-40} \text{erg s}^{-1}$ , and relatively high blackbody temperatures,  $T_{\text{in}} \sim 1.0 - 2.0 \text{keV}$ . From the constraint that  $L_x$  cannot exceed the Eddington luminosity,  $L_E$ , we require relatively high black-hole masses,  $M \sim 10 - 100 M_\odot$ , however, for such large masses the standard disk theory predicts lower blackbody temperatures,  $T_{\text{in}} < 1.0 \text{keV}$ . To understand a cause of this puzzling fact, we carefully calculate the accretion flow structure shining at  $\sim L_E$ , fully taking into account the advective energy transport in the optically thick regime and the transonic nature of the flow. Our calculations show that at high accretion rate ( $\dot{M} \gtrsim 30 L_E/c^2$ ) an apparently compact region with a size of  $R_{\text{in}} \simeq (1 - 3)r_g$  (with  $r_g$  being Schwarzschild radius) is shining with a blackbody temperature of  $T_{\text{in}} \simeq 1.8(M/10M_\odot)^{-1/4} \text{keV}$  even for the case of a non-rotating black hole. Further,  $R_{\text{in}}$  decreases as  $\dot{M}$  increases, on the contrary to the canonical belief that the inner edge of the disk is fixed at the radius of the marginally stable last circular orbit. Accordingly, the loci of a constant black-hole mass on the ‘‘H-R diagram’’ (representing the relation between  $L_x$  and  $T_{\text{in}}$  both on the logarithmic scales) are not straight but bent towards the lower  $M$  direction in the frame of the standard-disk relation.

We also plot the ASCA data of some ULXs on the same H-R diagram, finding that they all fall on the regions with relatively high masses,  $M \sim 10 - 30 M_\odot$ , and high accretion rates,  $\dot{M} \gtrsim 10 L_E/c^2$ . Interestingly, IC342 source 1, in particular, was observed to move along the constant- $M$  line (not constant  $R_{\text{in}}$  line) in our simulations. This provides a firm evidence that at least some ULXs are shining at  $\gtrsim L_E$ , and containing black holes with  $M \simeq 10 - 100 M_\odot$ .

*Subject headings:* accretion: accretion disks, black holes—stars: X-rays

## 1. INTRODUCTION

Already in the late 1980’s, *Einstein* satellite had found luminous X-ray sources with X-ray luminosities  $L_x \sim 10^{38-40} \text{erg s}^{-1}$  in nearby spiral galaxies (Fabbiano. 1989). They locate in the off-nucleus region of the host galaxy, hence cannot be an active-galactic nucleus (AGN) of low-luminosity. Only a small number of them are optically identified as young supernova remnants (e.g., the most luminous source in NGC 6946; Schlegel 1994), whereas we lack secure optical identifications for most of them. At present day, these luminous, non-AGN and non-supernova-remnant sources are called ‘‘Ultra Luminous X-Ray Sources (ULXs)’’ (see Makishima et al. 2000 and reference therein). Apparently, their X-ray luminosities greatly exceed the Eddington limit for a neutron star,  $\sim 2 \times 10^{38} \text{erg s}^{-1}$ , by a couple of orders of magnitude. ULXs are thus more like black-hole binaries (BHBs), although we need spectral information to reveal their emission mechanism.

Recently, much progress has been made on the study of ULXs. Thanks to the fine spectral and imaging capability of *ASCA*, high-quality spectra have been accumulated for numbers of ULXs, including NGC 1313 source A and B (Petre et al. 1994), M81 X-6 (Uno 1996), two ULXs in IC 342 (Okada et al. 1998), and so on. Especially, rather extensive study has been performed by Makishima et al. (2000) and Mizuno et al. (2000).

According to their study, the spectra of most ULXs in nearby galaxies can be well fitted with multi-color disk (MCD) model (Mitsuda et al. 1984), reinforcing its BHB interpretation. However, obtained disk temperatures, typically ranging 1.0–2.0 keV, somewhat contradict the BHB hypothesis. Theoretically, they are too high to be achieved by a standard-type disk around such a high-mass, Schwarzschild (non-rotating) black hole. They are also higher than those observed from well-studied Galactic/Magellanic BHBs (e.g., Tanaka & Lewin 1995). The observed high disk temperatures are hence the most severe problem regarding ULXs. To cope with this issue, some authors discussed the possibility of Kerr BH, although their arguments still remain rather qualitative. We need both the detailed calculation of spectra from BHBs and the careful comparison with the observations.

In this *Letter* we consider an important process which has not been fully appreciated in the study of ULXs. The accretion-disk theory predicts that for high luminosity, comparable to  $L_E$ , advective energy transport dominates over energy loss by radiation. Abramowicz et al. (1988) were first to construct such a disk model, currently known as the slim disk model (see also Szuszkiewicz et al. 1996; Wang et al. 1999). More recently, Watarai et al. (2000) and Mineshige et al. (2000) discussed the distinctive spectral features of the slim disks in connection with BHBs and narrow-line Seyfert 1 galaxies (NLS1s), respectively (see

<sup>1</sup> Department of Astronomy, Graduate School of Science, Kyoto University

<sup>2</sup> Department of Physics, Faculty of Science, Hiroshima University

<sup>3</sup> *E-mail* : watarai@kusastro.kyoto-u.ac.jp

also Fukue 2000). Following the same line, we calculate the structure and emission properties of high-luminosity accretion disks and demonstrate that the X-ray spectral properties of ULXs are indeed well understood by the slim disk model. In section 2 we give basic equations with advection, where we stress the necessity of solving flow structure with careful consideration of its transonic nature. We then show in section 3 the results of model fitting and compare the theory with ULXs observed by *ASCA*. In section 4, we argue that ULXs do really undergo super-critical accretion. The final section is devoted to conclusions. Throughout the present study, we normalize  $\dot{M}$  by  $L_E/c^2$  (with  $c$  being speed of light); i.e., the normalized mass-flow rate is  $\dot{m} \equiv \dot{M}/(L_E/c^2) \simeq \dot{M}/(1.4 \times 10^{17}(M/M_\odot) \text{ g s}^{-1})$ .

## 2. BASIC EQUATIONS AND NUMERICAL METHODS

The calculation code of the transonic accretion flow was first made by R. Matsumoto (see Matsumoto et al. 1984) and then modified by F. Honma and M. Takeuchi so as to incorporate the advected energy term. Basic equations used here are the same as those in the previous paper (Watarai et al. 2000). We assume: (1) the disk is steady ( $\partial/\partial t = 0$ ); (2) the disk is axisymmetric; (3) the Pseudo-Newtonian approximation (Paczynski & Wiita 1980) is adopted for a gravitational potential,  $\psi = -GM/(r - r_g)$  with  $r_g$  being the Schwarzschild radius; (4) the vertical disk structure is integrated.

The energy equation is symbolically written as  $Q_{\text{adv}}^- = Q_{\text{vis}}^+ - Q_{\text{rad}}^-$ , where the two terms on the R.H.S. represent viscous heating and radiative cooling, while the term on the L.H.S. is advection term (see Kato et al. 1988 for explicit expression).

We solved the full-set of the basic differential equations with semi-implicit method for appropriate boundary conditions. Black-hole accretion flow is transonic; it is subsonic far outside, whereas it is supersonic near the black hole. Thus, the solution should satisfy the regularity condition at the transonic point. The flow structure is calculated from the outer edge located at  $r_{\text{out}} = 10^4 r_g$  to  $r_g$  through the transonic point (barely inside  $\sim 3 r_g$ ). At the outer boundary, we impose the same physical quantities as those of the standard disk model, while at the inner boundary we assume torque-free conditions. For estimating the effective temperature, we assume the radiative cooling energy with black body radiation. For moderately large viscosity parameter,  $\alpha > 0.1$ , this assumption may break down (Beloborodov 1998), thus we assume relatively small  $\alpha = 0.01$  although spectra do not sensitively depend on  $\alpha$  (Watarai et al. 2000, in preparation; see also discussion in Mineshige et al. 2000). Then, the local effective temperature is  $T_{\text{eff}} = (Q_{\text{rad}}/2\sigma)^{1/4}$ . The Compton scattering within the disk will give rise to higher color temperature,  $T_{\text{col}} > T_{\text{eff}}$ . Such effects will be parameterized later. We assume the face on disk ( $i = 0$ ).

## 3. MODEL SPECTRAL FITTING

The MCD model has been very successful in analyzing soft X-ray spectra of low-mass X-ray binaries. However, it is valid only for the standard-type disks (with  $L \ll L_E$ ) in steady state, since it assumes that the temperature profile of the disk is  $T \propto r^{-3/4}$ . Mineshige et al. (1994) generalized the MCD model by setting the temperature gradient

to be  $T \propto r^{-p}$  with  $p$  being a fitting parameter. We use this “ $p$ -free model,” which is quite useful for discriminating slim disks showing  $p = 0.5$  from the standard one with  $p = 0.75$  (Watarai et al. 2000). Our fitting results of theoretically calculated spectra are summarized in Table 1.

Figure 1 displays the X-ray “H-R diagram” representing the relationship between X-ray luminosities and X-ray temperatures. In this figure, we plot the loci of constant  $M$  and constant  $\dot{M}$  based on the standard disk model (with dotted lines) and those based on our calculations (with solid lines). As was stated in Makishima et al. (2000), bolometric luminosity of the accretion disk is determined by the observational physical quantities,

$$L_{\text{bol}} = 7.2 \times 10^{38} \left( \frac{\xi}{0.41} \right)^{-2} \left( \frac{T_{\text{col}}/T_{\text{eff}}}{1.7} \right)^{-4} \times \left( \frac{R_{\text{in}}}{3r_g} \right)^2 \left( \frac{M}{10M_\odot} \right)^2 \left( \frac{T_{\text{in}}}{\text{keV}} \right)^4 \text{ erg s}^{-1}. \quad (1)$$

where  $\xi$  is a correction factor needed for the MCD model (Kubota et al. 1998), since the MCD model tends to overestimate the radius of the inner edge due to the negligence of the boundary term in the  $T_{\text{eff}}$  expression, and  $T_{\text{col}}/T_{\text{eff}}$  is a spectral hardening factor (Shimura & Takahara 1995), which relates the observed color temperature ( $T_{\text{col}}$ ) and effective temperature ( $T_{\text{eff}}$ ) of the disk. [Spectral hardening occurs because of internal Compton scattering, see Czerny & Elvis 1987; Ross, Fabian, & Mineshige 1992.] Note that normalized luminosity,  $\eta \equiv L/L_E$ , is mass-independent, as long as  $\dot{M}$  ( $\propto L$ ) is measured in a unit of  $L_E/c^2$ . When plotting our results in figure 1, we also include the corrections corresponding to  $\xi$  and  $T_{\text{col}}/T_{\text{eff}}$  above so that we can directly compare with the observational results using MCD approximation.

Clearly, our results roughly coincide with those of the standard disks in the low- $\dot{M}$  (lower-left) regions. A small discrepancy is due to the different adopted potentials: we used the pseudo-Newtonian potential, while the standard disk is based on the Newtonian one. In high- $\dot{M}$  regions, in contrast, our calculation results systematically shift towards the lower  $M$  direction in the frame of the standard-disk relation for given  $\dot{M}$ . This is due to the apparent shift of the inner boundary in transonic flows with high  $\dot{M}$ . The behavior of the two models on the X-ray H-R diagram is thus qualitatively distinct at high  $L$ .

In figure 1, we also plot *ASCA* observation results of ULXs and BHBs. Makishima et al. (2000) analyzed *ASCA* data of several ULXs and clarified their unique X-ray observational features at 0.5–10keV. We use the data sample of ULXs given by Mizuno et al. (2000), together with other samples of galactic sources from Makishima et al. (2000) for comparison (see Table 2). They show that ULXs tend to gather in the region with high  $M$  and  $L$ , compared with BHBs in figure 1.

We, here, pay particular attention to the multiple points of IC342 source 1 in figure 1, which indicate that this source moves along the constant- $M$  lines not of the standard disk but of the slim disk. Obviously, black-hole masses cannot change, while  $\dot{M}$  can on short timescales, say,  $< 1$  s. That is, the slim disk is more relevant here. Other objects, such as M81 X-8 and NGC1313 source B,

also move along our constant  $M$  lines. To see these more clearly, we plot in figure 2 the same quantities to those in figure 1 but on the  $R_{\text{in}}-T_{\text{in}}$  diagram. We can explicitly see in this figure how  $R_{\text{in}}$  changes as  $\dot{m}$  varies. These strongly support that we are actually observing changes in  $R_{\text{in}}$  in accord with variations in  $\dot{M}$ , which cannot be explained in the framework of the standard disk model.

#### 4. NATURE OF ULXS: REALLY UNDERGOING SUPER-CRITICAL ACCRETION?

The most common interpretation often made to explain high  $T_{\text{in}}$  and  $L$  of ULXs is that ULXs may contain Kerr black holes (Zhang et al. 1997). For Kerr holes, the marginally stable last circular orbit can be located at smaller radii, down to  $\sim 0.5r_{\text{g}}$  in an extreme case, thus yielding small  $R_{\text{in}}$  and, hence, high  $T_{\text{in}}$ . Also, the energy conversion efficiency from accretion energy to radiation energy can be as large as 0.42 at maximum, thereby generating large  $L$ .

However, we wish to stress that non-advective, non-transonic models are self-inconsistent in high  $\dot{M}$  regimes, because advective energy transport dominates over radiative cooling. We, in fact, see in figures 1 and 2 that typical accretion rates of ULXs are  $\dot{m} \simeq 30-100$ , for which a transition from the standard-type disk to the slim disk occurs. We can roughly express the disk luminosity as a function of  $\dot{m}$  (Watarai et al. 2000),

$$L(\dot{m}) \simeq L_{\text{E}} \begin{cases} 2[1 + \ln(\dot{m}/20)] & \text{for } \dot{m} \geq 20 \\ \dot{m}/10 & \text{for } \dot{m} < 20. \end{cases} \quad (2)$$

That is, we can expect significant advection effects for  $\dot{m} \gtrsim 20$ . Likewise, we expect significant amount of mass existing around inside the marginally stable last circular orbit. The similar situation may be realized in different circumstances, e.g. in the represent magnetic stress (Agol & Krolik 2000), in 2D numerical simulation (Stone et al. 1999), although there are no quantitative discuss have been made.

The distinction between the standard disk and the slim disk is not only quantitative but also qualitative. More important is that the Kerr model cannot account for time changes in  $R_{\text{in}}$ . In short, the peculiar behavior of some ULXs in figures 1 and 2 remain unexplained in the framework of usual disk models. It might be that there exists a slim disk surrounding a Kerr hole.

We assume the face on disk ( $i = 0$ ) and do not consider the relativistic effects, except for adopting the pseudo-Newtonian potential, in these figures. General relativistic (GR) effects (such as gravitational redshift, Doppler boosting, gravitational focusing due to ray bending) produce complex effects, depending on inclination angles. We calculate a slim disk model with face-on geometry, for which only gravitational redshift works, finding systematically larger  $R_{\text{in}}$  ( $\sim 3r_{\text{g}}$ ) by a factor of  $\sim 6$  and thus lower  $T_{\text{in}}$  ( $\sim 0.12$  keV) by a factor of  $\sim 2.5$  even for  $\dot{m} \gtrsim 100$ . In other words, most of radiation from inside  $3r_{\text{g}}$  vanishes for this case. For a face-on disk, therefore, GR effects cause decrease in  $T_{\text{in}}$  and increase in  $R_{\text{in}}$ , keeping roughly constant  $L$ . Corrections to remove Compton and GR effects from the data points are, hence,  $\Delta \log T_{\text{in}} \lesssim +0.4$  and  $\Delta \log R_{\text{in}} \lesssim -0.8$ .

For disks with non-zero inclination angles around a Schwarzschild black hole, Doppler boosting enhances radiation, yielding, at most, a factor of  $\sim 1.4$  increase in  $T_{\text{in}}$  compared with face-on disks, while the total flux kept roughly constant (Sun, Malkan 1989). We thus expect slight increase in  $T_{\text{in}}$  and decrease in  $R_{\text{in}}$  for a fixed  $R_{\text{in}}^2 T_{\text{in}}^4$  compared with face-on disks. Required corrections are  $\Delta \log T_{\text{in}} \lesssim -0.2$  and  $\Delta \log R_{\text{in}} \lesssim +0.4$ .

To summarize, the inclusion of GR and inclination effects cause large uncertainties in  $R_{\text{in}}$  and  $T_{\text{in}}$ . It then follows that we cannot obtain a good estimate of  $m$  and  $\dot{m}$  from figure 1, unless an inclination angle is accurately known. Nevertheless, our conclusion that ULXs are near critical accretion does not alter, since the positions of some ULXs in figures 1 and 2 really move along the qualitatively different path than that expected by the standard disk model. It is interesting to point that our calculations can well reproduce the observations, even without considering the GR and inclination effects. We also understand that sources such as IC342 source 1, M81 X-8, and NGC1313 source B cannot be face-on, for the reason that if so we do not expect  $R_{\text{in}}$  changes, since radiation from inside  $\sim 3 r_{\text{g}}$  will vanish.

#### 5. CONCLUSIONS

1. All the ULXs so far observed fall on the regions with high mass ( $M \sim 30M_{\odot}$ ) and high accretion rate ( $\sim 30L_{\text{E}}/c^2$ ) on the X-ray H-R diagram (figure 1).
2. The slim disk model predicts apparent decrease in  $R_{\text{in}}$  as  $L$  increases. This results in a qualitatively different evolutionary path of a single object on the X-ray H-R diagram, compared with that of the standard disk (i.e., constant  $R_{\text{in}}$  line). ULXs that are observed at several different epochs (only IC342 was observed at same epochs) actually follow the constant- $M$  lines of the slim disk, not those of the standard disk. This provides a firm evidence that at least some ULXs are near critical accretion phase.
3. It is not always clear whether a central black hole is rotating or not. What we can conclude is that high luminosity,  $\sim L_{\text{E}}$ , is realized in ULXs, not depending on the nature of black holes.
4. In future work, we need more accurate evaluations of GR effects and the effects of changing viscosity prescriptions. Also, more extensive observational studies, particularly independent estimates of inclination angles, are indispensable for fully understanding the nature of ULXs.

We would like to thank Dr. K. Makishima for useful comments and discussions. This work was supported in part by the Grants-in Aid of the Ministry of Education, Science, Sports, and Culture of Japan (10640228, SM).

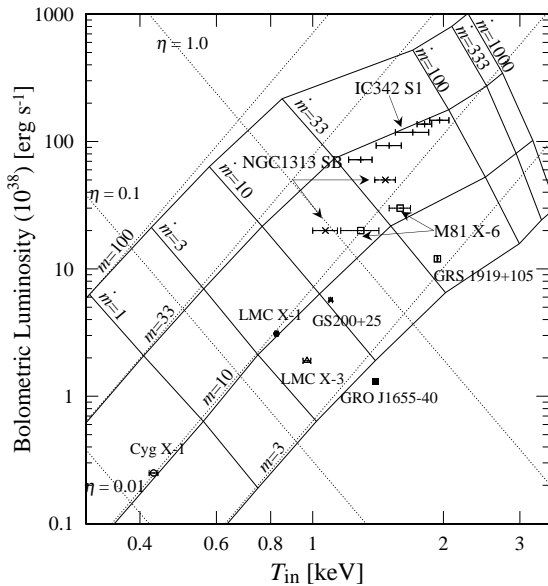


FIG. 1.— X-ray H-R diagram of X-ray sources. Solid lines represent the constant  $m$  (black-hole mass) and constant  $\dot{m}$  loci according to our model, while dotted lines are the same but based on the standard accretion disk (SSD) theory. When calculating both lines, the boundary ( $\xi$ ) and Compton ( $T_{\text{col}}/T_{\text{eff}}$ ) effects are both included. Other symbols denote the *ASCA* data of ULXs and BHBs taken from Mizuno (2000) and Makishima et al. (2000). The inclination angle is assumed to be  $i=0$  (face on).

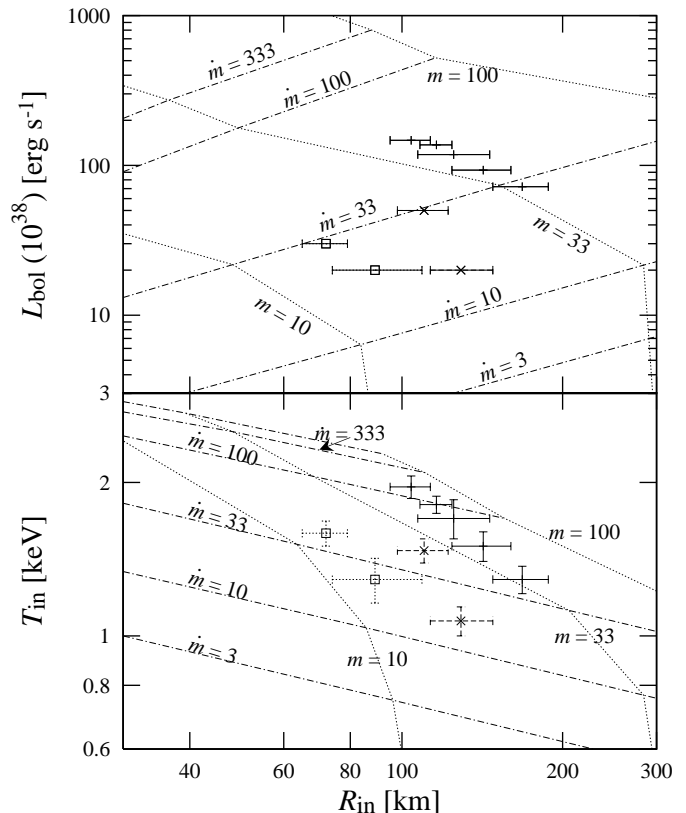


FIG. 2.— The same as figure 1 but on the  $R_{\text{in}}-L_{\text{bol}}$  (bolometric luminosity),  $R_{\text{in}}-T_{\text{in}}$  diagram. Dotted and dash-dotted lines represent the constant  $m = M/M_{\odot}$  and  $\dot{m}$ , respectively.

## REFERENCES

- Abramowicz, M.A., Czerny, B., Lasota, J.P., Szuszkiewicz, E. 1988, *ApJ*, 332, 646  
 Agol, E., Krolik, J.H. 2000, *ApJ*, 528, 161  
 Beloborodov, A.M. 1998, *MNRAS*, 297, 739  
 Colbert, E.J.M., Mushotzky, R.F. 1999, *ApJ*, 519, 89  
 Czerny, B., Elvis, M. 1987, *ApJ*, 321, 305  
 Fukue, J. 2000, *PASJ*, in press  
 Fabbiano, G. 1989, *A&A Rev.*, 27, 87  
 Kato, S., Fukue, J., Mineshige, S. 1998, *Black-Hole Accretion Disks* (Kyoto University Press, Kyoto)  
 Kubota, A., Tanaka, Y., Makishima, K., Ueda, Y., Dotani, T., Inoue, H., Yamaoka, K. 1998, *PASJ*, 50, 667  
 Makishima, K et al. 2000, *ApJ*, 535, 632  
 Matsumoto, R., Kato, S., Fukue, J., Okazaki, A. 1984, *PASJ*, 36, 71  
 Mitsuda, K. et al. 1984, *PASJ*, 36, 741  
 Mineshige, S., Hirano, A., Kitamoto, S., Yamada, T.T., Fukue, J. 1994, *ApJ*, 426, 308  
 Mineshige, S., Kawaguchi, T., Takeuchi, M., Hayashida, K. 2000, *PASJ*, 52, 499  
 Mizuno, T., Ohnishi, T., Kubota, A., Makishima, K., Tashiro, M. 1999, *PASJ*, 51, 663  
 Mizuno, T et al. 2000 (in preparation)  
 Paczyński, B., Wiita, P.J. 1980, *A&A*, 88, 23  
 Petre, R., Okada, K., Mihara, T., Makishima, K., Colbert, E.J.M. 1994, *PASJ*, 46, L115  
 Ross, R.R., Fabian, A.C., Mineshige, S. 1992, *MNRAS*, 258, 189  
 Schlegel, E.M. 1994, *ApJ*, 424, L99  
 Shakura, N.I., Sunyaev, R.A. 1973, *A&A*, 24, 337  
 Shimura, T., Takahara, F. 1995, *ApJ*, 445, 780  
 Stone, J.M., Pringle, J.E., Begelman, M.C. 1999, *MNRAS*, 310, 1002  
 Szuszkiewicz, E., Malkan, M.A., Abramowicz, M.A. 1996, *ApJ*, 458, 474  
 Sun, W.-H., Malkan, M.A. 1989, *ApJ*, 346, 68  
 Tanaka, Y., Lewin, W. H. G. 1995, in *X-ray Binaries*, ed W. H. G. Lewin, J. van Paradijs, W. P. J. van den Heuvel (Cambridge University Press, Cambridge) p126  
 Uno, S., Annual Meeting of Astronomical Society of Japan, 1996, Spring, R40a  
 Wang, J.M., Szuszkiewicz, E., Lu F.J., Zhou Y.Y., 1999, *ApJ*, 522, 839  
 Watarai, K., Fukue, J. 1999, *PASJ*, 51, 725  
 Watarai, K., Fukue, J., Takeuchi, M., Mineshige, S. 2000, *PASJ*, 52, 133  
 Zhang, S.N., Cui, W., Chen, W. 1997, *ApJ*, 482, L155  
 Zhang, S.N., et al. 1997, *ApJ*, 479, 381

TABLE 3  
FITTING RESULTS OF P-FREE MODEL (0.2-10keV) ( $M = 33M_{\odot}$ )

$\dot{M}/(L_E/c^2)$	$T_{\text{in}}$ (keV)	$R_{\text{in}}$ (km)	p
1	0.24(0.2-3.0 keV)	758.6	0.73
3	0.33(0.2-5.0 keV)	724.4	0.73
10	0.45	691.8	0.72
33	0.66	501.2	0.67
100	1.21	165.9	0.59
333	1.48	117.5	0.55
1000	1.61	95.5	0.53

TABLE 4  
FITTING RESULTS OF ULXs WITH ASCA (0.5-10keV)

Source	$T_{\text{in}}$ (keV)	$R_{\text{in}}$ (km)	$L_{\text{bol}}$ ( $10^{38}$ erg s $^{-1}$ )
IC342 source 1	1.96 $\pm$ 0.1	104 $\pm$ 9	147
	1.5 $\pm$ 0.1	142 $\pm$ 18	93
	1.7 $\pm$ 0.15	125 $\pm$ 21	118
	1.29 $\pm$ 0.08	168 $\pm$ 20	72
	1.81 $\pm$ 0.07	116 $\pm$ 8	137
NGC1313 source B	1.47 $\pm$ 0.08	110 $\pm$ 12	50
	1.07 $\pm$ 0.07	129 $^{+19}_{-16}$	20
M81 source X6	1.59 $\pm$ 0.09	72 $\pm$ 7	30
	1.29 $\pm$ 0.13	89 $^{+20}_{-15}$	20